Pergamon

Cement and Concrete Research 30 (2000) 1395–1400

CEMENT AND CONCRETE RESEARCH

Electrical conductivity, diffusion, and permeability of Portland cement-based mortars

W.J. McCarter*, G. Starrs, T.M. Chrisp

Department of Civil and Offshore Engineering, Heriot Watt University, Edinburgh EH14 4AS, Scotland, UK

Received 1 September 1999; accepted 11 April 2000

Abstract

The electrical conductivity of a range of Portland cement-based mortars was studied over a period of 450 days hydration. The influence of thermal cycling on conductivity was investigated and the activation energy, E_a, established for conduction processes. E_a was found to be system specific and was in the range 16–30 kJ/mol (0.16–0.31 eV/ion); pozzolanic additions had the effect of increasing E_a in comparison with the plain ordinary Portland cement (OPC) mortar. Results also indicate that on the initial heating cycle, microstructural changes occurred. At the end of the test period, permeability and diffusion tests were carried out and data are presented in this respect.

Keywords: Hydration; Characterization; Electrical properties; Blended cements; Arrhenius relationship

1. Introduction

Characterization of the developing microstructure within cementitious systems represents an important area, and a variety of techniques have now been exploited in this respect. These include, for example, scanning electron microscopy, mercury intrusion porosimetry, magic angle spinning and small angle X-ray scattering. The continuously evolving pore network is critical in all aspects of the science of cement-based materials including strength, permeability, diffusion, sorptivity, leaching, creep and shrinkage. Electrical property measurements, as applied to cementitious materials, represent an additional and still developing investigative technique in the study of these materials both at the micro- and macro-scale (see, for example, references [1–8]). From an engineering point of view, there is a need to be able to characterize the capillary pore network using easily measured properties and, to this end, electrical measurements could be exploited.

The current work investigates the electrical conductivity of a range of Portland cement-based binders over a 450-day time scale; in particular, the influence of thermal cycling on electrical measurements of mature cementitious systems formed an important aspect of the investigation. Regarding the latter, there is a dearth of information in this area. At the end of the test period, a more limited series of tests was undertaken on water permeability and chloride diffusion.

2. Experimental

2.1. Test specimens

The oxide analysis of the materials employed within the experimental program is presented in Table 1. Ordinary Portland cement (OPC) was used throughout. The pozzolanic materials comprised ground granulated blast-furnace slag (GGBS), metakaolin (MK), and micro-silica (MS). Mortar samples were used throughout and are presented in Table 2; the fine aggregate (i.e. <5 mm maximum size) conformed to grading zone M as defined in BS882: 1992 [9]. Materials were initially dry-mixed in a Hobart planetary motion mixer (10 l capacity) for 2 min; distilled water was added and mixing continued for a further 5 min and subsequently compacted in steel moulds. Samples were prepared as 100 × 60 mm (diameter) cylinders, demoulded at 24 h and stored in 100% RH (at 20°C) thereby avoiding leaching problems associated with submerged curing. A total of 10

* Corresponding author. Tel.: +44-131-451-3318; fax: +44-131-451-5078.

E-mail address: johnm@civ.hw.ac.uk (W.J. McCarter).

0008-8846/00/$ – see front matter
PII: S0008-8846(00)00281-7

cylinders were cast for each mix in Table 2. Undertaken were 28-day compressive strength tests (denoted F_{28}) of 75 mm cubes (mean of three cubes) and presented in Table 2. A further series of cylinders was cast for pore-fluid conductivity studies (six per mix).

Test specimens for electrical measurements took the form of disks 15 mm thick and 60 mm in diameter cut from the central region of these larger cylinders at the time of testing. Electrical measurements were taken at 3, 14, 28, 90 and 450 days.

2.2. Impedance measurements

Stainless steel disc electrodes were cemented onto the disk-specimens using a silver-loaded conductive paint. Complex impedance measurements were obtained using a Solartron 1260 frequency response analyser operating over the frequency range 100 Hz–10 MHz with a signal amplitude of 100 mV. Open-, short-, and load-calibration (using a precision capacitor and resistor) were performed at each test frequency. Such measurements allowed accurate identification of the bulk conductance [1] of the specimen that was subsequently converted to sample conductivity (σ_{bulk}).

At 450 days, the specimens were also subjected to a temperature cycling regime. For these measurements, specimens were placed in a temperature controlled, environmental chamber. The chamber was initially at 20°C and taken incrementally through the cycle from 20°C up to 50°C then down to 10°C and back to 50°C, etc. This repeated itself three times with 100% RH being maintained throughout. Samples were held at each temperature for 2 days before initiating impedance measurements thereby ensuring that no temperature gradients existed through the specimens.

Conductivity measurements were undertaken on the pore fluid (σ_{pore}) extracted from the mortar cylinders using a high-pressure pore press. Technical difficulties were encountered in expressing sufficient pore fluid from the sample at hydration times in excess of approximately 4 weeks; as a consequence, data were only obtained at 3, 14, and 28 days.

2.3. Diffusion and permeability measurements

Diffusion tests were undertaken at 450 days representing a relatively mature system and reducing the influence of hydration and pozzolanic activity to a minimum. A divided-cell technique [10–12] was used to study the diffusion of Cl^-. Cells (three per mix) were placed in a water bath at 20°C and the effective diffusivity, D_{eff}, of the Cl^- ion calculated from the steady state increase with time of the Cl^- concentration in the solution on the 'low' concentration side of the cell. The high concentration side of the cell contained a 1.0 M NaCl solution.

Water permeability measurements were obtained on disk specimens as detailed above (two per mix). The curved surface of the specimens was prepared with an epoxy-resin 'sleeve' and then placed in a permeability test rig [13]. A water pressure equivalent 100-m head of water was applied to the bottom surface of the specimen and the linear volumetric increase with time on the 'low-pressure' side of the sample monitored.

Table 1
Oxide analysis of materials used in the experimental programme

% By weight	OPC	MS	MK	GGBS
SiO_2	20.68	92.0	55.40	34.33
Al_2O_3	4.83	1.0	40.50	12.60
Fe_2O_3	3.17	1.0	0.65	0.60
CaO	63.95	0.3	0.01	41.64
MgO	2.53	0.6	0.12	8.31
K_2O	0.54	0.8	1.00	0.47
Na_2O	0.08	0.3	0.13	0.25

Table 2
Mix ratios of mortars (relative to Mix 1 datum; binder comprises OPC and replacement)

Materials	Mix 1	Mix 2	Mix 3	Mix 4	Mix 5
OPC	1	0.5	0.8	0.8	0.5
GGBS	+	0.5	+	+	0.3
MK	+	+	0.2	+	0.2
MS	+	+	+	0.2	+
Fine aggregate	3	3	3	3	3
Water/binder ratio (by mass)	0.55	0.55	0.55	0.55	0.55
F_{28} MPa	19	16	26	22	21

3. Discussion of results

3.1. Bulk conductivity (at 20°C)

The decrease in bulk conductivity, σ_{bulk}, over the 450-day test period is presented in Fig. 1A. In comparison with the plain OPC mix (Mix 1), the conductivity of the mixes with pozzolanic additions decreases more rapidly over the initial 28-days (particularly Mixes 3 and 5) and, in the longer term, achieve a lower value than Mix 1. This reflects the influence of the pozzolanic reaction. The decrease in conductivity of the saturated specimens will result from two sources,

(a) a reduction in connected capillary porosity due to a refinement in the pore structure, and
(b) changes in ionic concentrations within the pore fluid.

Regarding (b), this has been found to be particularly significant in the case of silica fume based binders where the conductivity of the pore water can reduce considerably over the period 28–365 days [14].

Pore-fluid conductivity measurements were taken on samples, although as noted in the Experimental section above, were confined to the initial 28-days hydration. Fig.

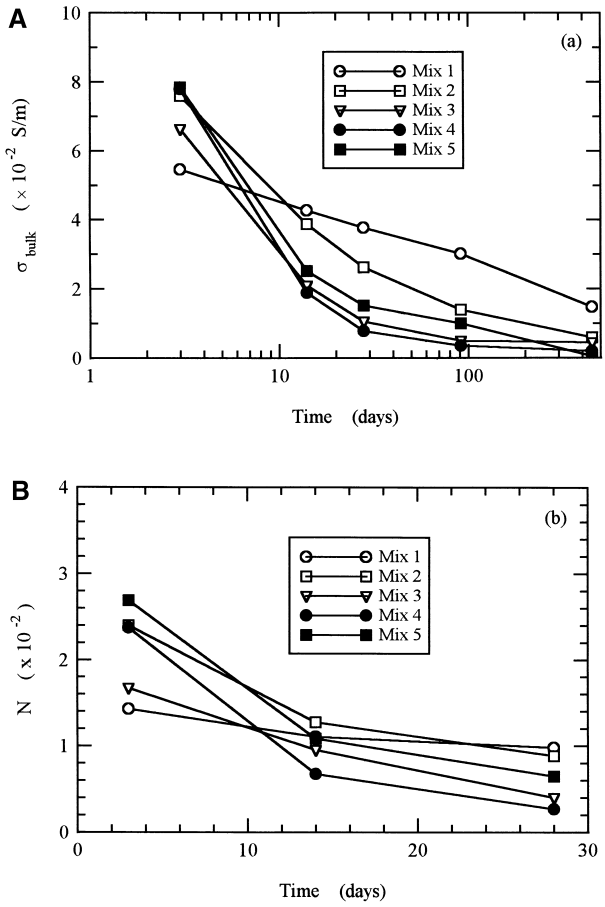

Fig. 1. (A) Decrease in bulk conductivity over the test period; and (B) variation in normalised conductivity, N, over the initial 28 days.

1b presents the normalised conductivity, N, over the initial 28-days hydration where N is defined in Eq. (1),

$$N = \frac{\sigma_{\text{bulk}}}{\sigma_{\text{pore}}}. \quad (1)$$

In this format, the relative effects of changing microstructure and pore-fluid conductivity can be assessed. Since N decreases with time, this implies that the bulk conductivity is decreasing at a faster rate than changes in pore-fluid conductivity. Microstructural changes (e.g. increasing pore tortuosity, pore constriction) are thus exerting a more dominant effect on the measured conductivity than pore-fluid chemistry. Whereas for an individual mix the conductivity of the pore fluid changes by less than a factor of two over the 28-day period, the bulk conductivity can, in some instances, decrease by almost an order of magnitude (i.e. Mix 4). The parameter, N, thus allows comparison of the changing pore network of different binders.

3.2. Bulk conductivity vs. temperature

The influence of thermal cycling on the bulk conductivity of mature mortar samples (450 days old) is presented in Fig. 2A–E. The temperature was cycled over the range 10–50°C. For comparative purposes, Fig. 3 presents the conductivity of a pore fluid over the temperature range 10–50°C. Figs. 2 and 3 are presented in the Arrhenius format in Eq. (2),

$$\sigma_{\text{bulk}} = A\mathrm{e}^{-\left[\frac{E_a}{RT}\right]} \quad (2)$$

where A is a pre-exponential constant; R is the gas constant (8.314 J/K mol); T is the absolute temperature (K) and E_a, the activation energy for the conduction process.

The mortar samples are taken around three temperature cycles with each cycle comprising an increasing (I) and decreasing (D) portion (denoted T1-I; T1-D; T2-I, etc. on legend). It is evident that in the increasing portion of the first cycle an anomaly occurs at 40°C ($1000/T = 3.19$/K) whereby the slope of the Arrhenius plot alters. This feature is most prominent in the plain OPC mortar, but is evident in all mixes. This feature becomes less significant with subsequent increasing temperature cycles. In the decreasing portion of the temperature cycle, no such anomaly occurs.

The activation energy (E_a) obtained from each Arrhenius plot is presented in the figure legend for both increasing and decreasing portions of each temperature cycle. Concerning the increasing temperature, the activation energy is calculated only in that portion of the conductivity data up to 40°C. The pre-exponential constant is not presented as measurements of conductivity were confined to a narrow range of temperatures and significant errors could be incurred in extrapolating the Arrhenius plot to $1/T = 0$. The activation energy in the cooling portion of the thermal cycle is less than that in the respective heating portion for all mixes. At this stage, this difference may not be that significant considering the uncertainty in the derived activation energy.

It is evident that the addition of pozzolanic materials generally increases the activation energy relative to the plain OPC mix (Mix 1). The system with the highest activation is represented by the ternary blended binder (Mix 5) and its is noteworthy that the activation energy is higher than either of the respective binary blended systems (Mix 2 and Mix 3). The activation energy for free pore fluid in Fig. 3 is 13.8 kJ/mol (0.14 eV/ion) and this is less than that of the mortar systems. It is recognised that pozzolanic materials result in a finer, more tortuous pore network than that of a plain OPC; reduced ionic mobility, ion–ion interaction and surface forces operative within the confines of the pore network must result in the (electrical) behaviour of the pore fluid differing from that of the free electrolyte.

There are limited data on the influence of thermal effects on activation energy for electrical conduction processes in Portland cement-based mortars. Data have been published for 28-day old neat OPC pastes [11] with a water/binder ratio = 0.4 taken around one temperature cycle: 30°C up to 60°C and back to 20°C. The entire

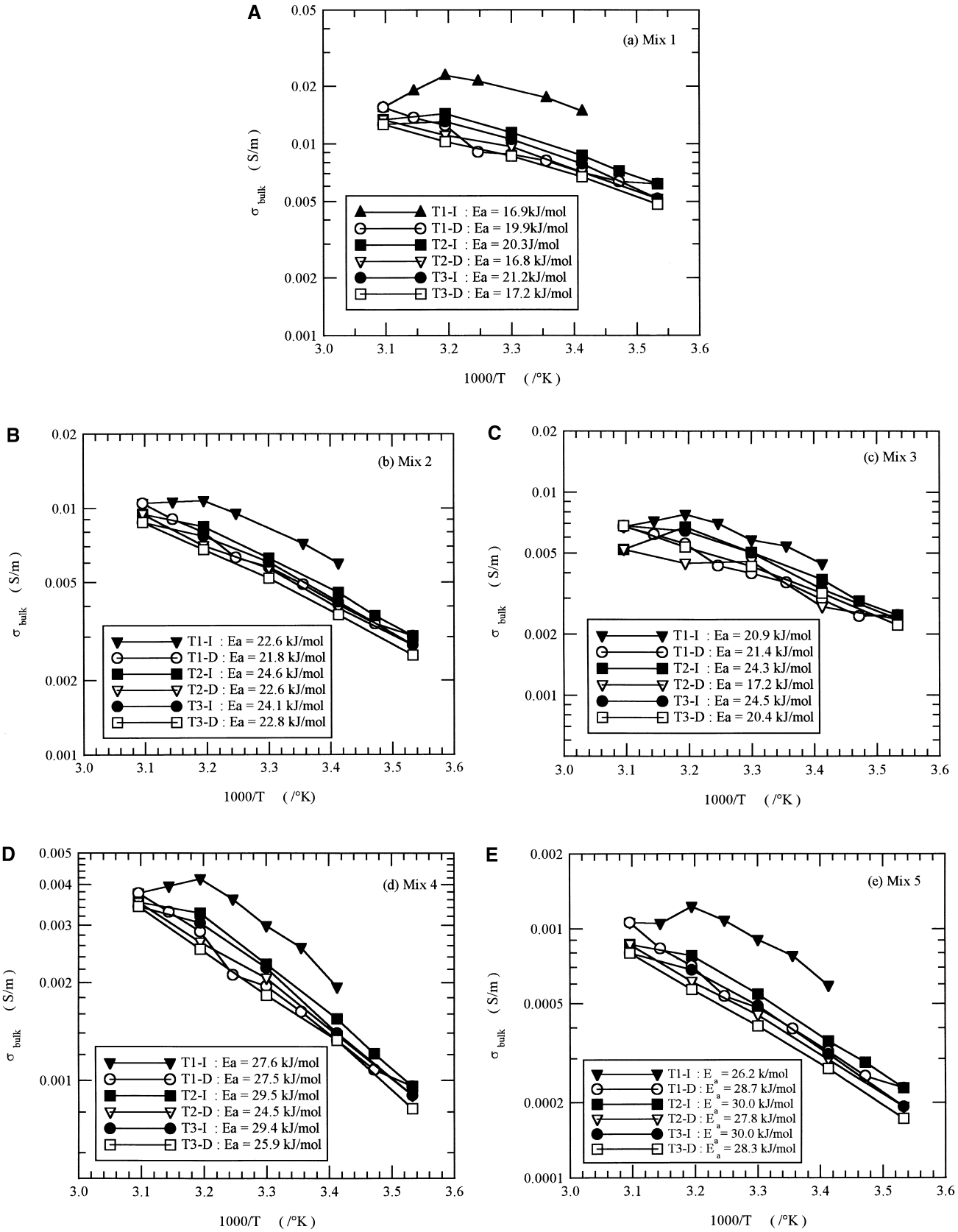

Fig. 2. Arrhenius plots over three thermal cycles for (A) Mix 1; (B) Mix 2; (C) Mix 3; (D) Mix 4; and (E) Mix 5 (Note: each cycle is denoted T1, T2, and T3; and each cycle comprises an increasing portion (denoted I) and a decreasing portion (denoted D)).

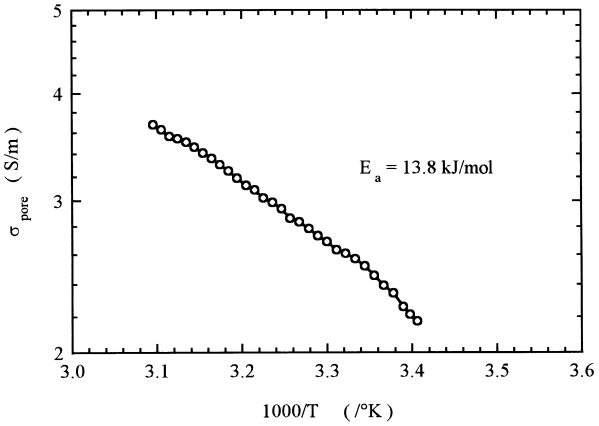

Fig. 3. Arrhenius plot for pore fluid taken over the temperature range 20–50°C.

cycle completed within a period of 10 h and the E_a value for the paste was 27.6 kJ/mol (0.29 eV/ion) for increasing temperature and 23.6 kJ/mol (0.24 eV/ion) for decreasing temperature. E_a for a mature OPC mortar with a water/binder ratio = 0.4 and a sand/cement ratio of 3:1, undergoing a single increasing temperature regime, has been quoted as 19.4 kJ/mol (0.20 eV/ion) over the range 10–40°C [15].

Increasing the temperature of the mortar specimens can result in a number of synergistic and opposing effects, for example,

(a) from Fig. 3, the conductivity of the free pore fluid displays a natural temperature dependence, increasing with increasing temperature;
(b) within the pore network, the chemical composition of the pore fluid may change due to changes in solubility of the mineralogical phases. Dissolution would increase ionic concentration within the pore fluid thereby increasing its conductivity; and,
(c) microstructural changes, resulting in a reduction in the connected porosity, would have the effect of decreasing bulk conductivity.

Fig. 2 would suggest that at temperatures in excess of approximately 40°C, the decrease in bulk conductivity resulting from microstructural changes ((c) above) must exert a greater influence than the combined effects of (a) and (b). This feature is only significant in the initial heating cycle. It is noteworthy that Joule heating effects [16] cause an increase in resistivity (reciprocal of conductivity) of Portland cement systems and has, in part, been attributed to changes in microstructure.

3.3. Diffusion, permeability, and conductivity (at 20°C)

The diffusivity and permeability of hardened mortars depend upon the pore structure although in different ways. These coefficients have been related to the measured conductivity through, respectively, the Nernst–Einstein relationship and the Katz–Thompson equation. The Nernst–Einstein has been applied to cementitious materials [2,4,17–19] in the form,

$$\frac{\sigma_{\text{bulk}}}{\sigma_{\text{pore}}} \approx \frac{D_{\text{eff}}}{D_{\text{o}}} = Q \tag{3}$$

where D_o is the diffusivity of the species at infinite dilution; D_{eff}, the effective diffusivity of the same species in the mortar, and Q is termed the diffusibility of the medium. The normalised conductivity, N, discussed above and presented in Fig. 1a, would represent the change in diffusibility with time for the mortar mixes. The use of Eq. (3) to predict D_{eff} from conductivity measurements may only be valid provided a suitable value of D_o is chosen and employing the value of the species at infinite dilution may be inappropriate [18]. A recent study has developed relationships for specific types of binders showing that a resistivity measurement may, on its own, be sufficient to estimate diffusion coefficient [20].

Regarding permeability, the Katz–Thompson approach [21] involves two microstructural parameters: a characteristic length scale and a measure of the pore-system connectivity. The characteristic length has been obtained as the threshold pore diameter, d_c, obtained from MIP tests and the pore connectivity is obtained from $\sigma_{bulk}/\sigma_{pore}$ as defined above. The equation employed is of the form,

$$k = \frac{1}{226}\frac{\sigma_{\text{bulk}}}{\sigma_{\text{pore}}} d_{\text{c}}\left(\frac{\rho g}{\eta}\right) \tag{4}$$

where k is the permeability in m/s; ρ is the density of water; g is the gravitational acceleration and η, the viscosity of the permeating fluid. The general applicability of such an approach has been criticised [22]. Some limited studies [23] utilising both MIP and conductivity data on young cement pastes (i.e. <28 days old) indicate reasonable agreement with Eq. (4) above although conflicting results have been published [24,25].

Unfortunately, we were unable to obtain the pore-fluid conductivity of mature mortars as used in our experimental programme. It is recognised that in the long term, binders such as MS show an appreciable decrease in pore-fluid concentration which, in addition to pore refinement, will serve to reduce conductivity. A conductivity measurement on its own may thus only allow a relative assessment

Table 3
Values of effective Cl^- diffusion coefficient (D_{eff}), water permeability (k), and bulk conductivity (σ_{bulk}) of mortars determined after 450 days (20°C)

Mix	$D_{eff} \times 10^{-12}$ (m^2/s)	$k \times 10^{-13}$ (m/s)	$\sigma_{bulk} \times 10^{-3}$ (S/m)
1	2.42	30.5	14.4
2	0.45	8.54	6.0
3	0.41	3.42	4.4
4	0.38	5.23	2.0
5	0.14	1.21	0.6

of mass transport and flow coefficients for similar binder types and not generally. For comparative purposes, Table 3 presents the effective diffusion coefficient and permeability for all mixes, together with their measured conductivity, σ_{bulk}.

4. Concluding comment

In the current work, the electrical conductivity of a range of cementitious binders was studied over 450 days. Bulk conductivity measurements on mortars and their respective pore fluids indicate that over the initial 28-days hydration, changes in the pore structure exerted a greater influence on the measured conductivity than changes in pore-fluid conductivity. At the end of the test period, Arrhenius plots were established for the conduction process under a thermal cycling regime and represents an area where there is a dearth of published data. The activation energy was found to be binder specific.

Acknowledgments

The Authors wish to thank the Engineering and Physical Sciences Research Council (EPSRC) for financial support (Grant Reference GR/K65089). Thanks are also expressed to Dr. H. Ezirim and Mr. H. Barras for their assistance in the experimental work.

References

[1] W.J. McCarter, R. Brousseau, The AC response of hardened cement paste, Cem Concr Res 20 (6) (1990) 891–900.
[2] C. Andrade, C. Alonso, S. Goni, Possibilities for electrical resistivity to universally characterise mass transport processes in concrete, in: R.K. Dhir, M.R. Jones (Eds.), Proc. of the Concrete 2000 Conf., Dundee, Sept., 1993 vol. 2, E&FN Spon, 1993, pp. 1639–1652.
[3] P. Gu, P. Xie, Z. Xu, J.J. Beaudoin, A rationalized AC impedance model for microstructural characterisation of hydrating cement systems, Cem Concr Res 23 (2) (1993) 359–367.
[4] B.J. Christensen, R.T. Coverdale, R.A. Olsen, S.J. Ford, E.J. Jennings, T.O. Mason, Impedance spectroscopy of hydrating cement-based materials: Measurement, interpretation, and applications, J Am Ceram Soc 77 (11) (1994) 2789–2804.
[5] E.J. Garboczi, L.M. Schwartz, D.P. Bentz, Modelling the D.C. electrical conductivity of mortar, Mater Res Soc Symp Proc 370 (1995) 429–436.
[6] W.J. McCarter, The a.c. impedance response of concrete during early hydration, J Mater Sci 31 (1996) 6285–6292.
[7] P.J. Tumidajaski, A.S. Schumacher, S. Perron, J.J. Beaudoin, On the relationship between porosity and electrical resistivity in cementitious systems, Cem Concr Res 26 (4) (1996) 529–534.
[8] S.L. Cormack, D.E. MacPhee, D. Sinclair, An AC impedance spectroscopy study of hydrated cement pastes, Adv Cem Res 10 (4) (1998) 150–151.
[9] British Standards Institution, BS812, Part 103, Methods for determination of particle size distribution, London, 1985.
[10] C.L. Page, N.R. Short, A. El-Tarras, Diffusion of chloride ions in hardened cement pastes, Cem Concr Res 11 (3) (1981) 383–394.
[11] A. Atkinson, A.K. Nickerson, The diffusion of ions through water-saturated cement, J Mater Sci 19 (1984) 3068–3078.
[12] N.R. Buenfeld, J.Z. Zhang, AC impedance study of sealer- and coating-treated mortar specimens, Adv Cem Res 10 (4) (1998) 169–178.
[13] P. Bamforth, The water permeability of concrete and its relationship with strength, Mag Concr Res 43 (157) (1991) 233–241.
[14] C. Shi, J.A. Stegemann, R.J. Caldwell, Effect of supplementary cementing materials on the specific conductivity of pore solution and its implications on the rapid chloride permeability test (AASHTO T277 and ASTM C1202) results, Am Concr Inst Mater J 95 (4) (1998) 389–394 July/August.
[15] W.J. McCarter, Effects of temperature on conduction and polarization in Portland cement mortar, J Am Ceram Soc 78 (2) (1995) 411–415.
[16] Z. Liu, J.J. Beaudoin, An assessment of the relative permeability of cement systems using A.C. impedance techniques, Cem Concr Res 29 (7) (1999) 1085–1090.
[17] A.A. Kyi, B. Batchelor, An electrical conductivity method for measuring the effects of additives on effective diffusivities in Portland cement pastes, Cem Concr Res 24 (4) (1994) 752–764.
[18] P.J. Tumidajski, A.S. Schumacher, On the relationship between the formation factor and propan-2-ol diffusivity in mortars, Cem Concr Res 26 (9) (1996) 1301–1306.
[19] X. Lu, Application of the Nernst–Einstein equation to concrete, Cem Concr Res 27 (2) (1997) 293–302.
[20] K.O. Ampadu, K. Torii, M. Kawamura, Beneficial effect of fly ash on chloride diffusivity of hardened cement paste, Cem Concr Res 29 (4) (1999) 585–590.
[21] A.J. Katz, A.H. Thompson, Quantitative prediction of permeability in porous rock, Phys Rev B: Condens Matter 34 (11) (1986) 8179–8181.
[22] J.P. Ollivier, M. Massat, Permeability and microstructure of concrete: a review of modelling, Cem Concr Res 22 (2/3) (1992) 503–514.
[23] B.J. Christensen, T.O. Mason, H.M. Jennings, Comparison of measured and calculated permeabilities for hardened cement pastes, Cem Concr Res 26 (9) (1996) 1325–1334.
[24] S. El-Dieb, R.D. Hooton, Evaluation of the Katz–Thompson model for estimating the water permeability of cement-based materials from mercury intrusion porosimetry, Cem Concr Res 24 (3) (1994) 443–455.
[25] P.J. Tumidajski, B. Lin, On the validity of the Katz–Thompson equation for permeabilities in concrete, Cem Concr Res 28 (5) (1998) 643–647.